

Open-loop printing of liquid metal for the low-cost rapid fabrication of soft sensors

Junda Chen¹, Benjamin Shih², Iman Adibnazari¹, Yong-Lae Park³, Michael Tolley¹

Abstract—Soft sensors consisting of highly conductive liquid metal, eutectic gallium-indium (eGaIn), embedded in a soft elastomer have been of great interest recently due to their stretchability for sensing temperature, pressure, and strain for a variety of applications. Previous studies have explored methods for patterning the liquid metal during the manufacture of soft sensors. Among these, direct printing of eGaIn is attractive as it is easily re-configurable for fabricating custom sensors. However, to print liquid metal traces with consistent widths, previous approaches require combinations of 1) high-precision feedback control of the stand-off distance and the extrusion rate, 2) a very low stage velocity, and/or 3) modification of the properties of liquid metal with additional components or processing steps. To address these limitations, we present two open-loop liquid metal printing methods to achieve high precision using a low-cost, open-source system without the need to optimize the properties of the liquid metal. We discuss how key print parameters—as well as a novel print head design inspired by a paintbrush—affect the printing quality, and how well the printing methods can resist variation in the height of the substrate. We then apply these methods to manufacture soft strain sensors, which we test and calibrate. In general, these printing methods represent easily accessible methods for manufacturing liquid metal sensors without the need for complex equipment or materials processing.

I. INTRODUCTION

Soft sensors have recently grown in popularity due to their higher compliance, deformability, and robustness compared to many rigid sensors. There are various types of soft sensors including capacitive sensors with dielectric layers of conductive polymers [1], [2], capacitive and resistive sensors using polydimethylsiloxane (PDMS) with structured carbon black [3], [4], sensors using stretchable optical fibers [5], [6], sensors using carbon nanotubes [7], [8] and 3D printed sensors consisting of layers of nonconductive and conductive photopolymers [9].

Among these soft sensors, liquid metal sensors using eutectic Gallium-Indium (eGaIn) are frequently used because of the high conductivity of eGaIn, which maintains electrical connection even with large deformation. The liquid state of eGaIn at room temperature enables the development of flexible sensors that are more conducive to use in wearable devices when compared to soft sensors based on solid-state conductors. Many researchers have recently reported various types of liquid metal sensors, including tactile sensors for measuring both temperature and contact force [10], soft skin

with sensor arrays that can distinguish different types of external contacts using machine learning [11]–[13], multi-axis force sensors that can decouple normal force from shear force [14], multi-modal sensors that can simultaneously sense strain deformation and pressure [15], and multi-modal gloves that can monitor the motions of human hands to provide haptic and thermal feedback based on the activities of a user in virtual reality (VR) [16].

Previous work explored various methods for patterning liquid metal during manufacturing of soft sensors and stretchable electronics, including direct printing [17]–[20], injection into patterned microchannels [15], lithography [21], and spraying over stencils [22]. However, methods, such as injection, lithography, and spraying, often require complex steps during manufacturing, long manufacturing cycles, and expensive equipment. For injection, manufacturers first needed to assemble two layers of elastomer made by two different molds into a sensor with empty embedded channels, then inserted a syringe needle into one end of the channel to inject liquid metal, and another syringe needle into the other end to simultaneously remove air from the channel [15]. While effective, this manufacturing process required considerable skill and manual labor, limiting the scalability of this approach. An alternative approach used lithography to pattern liquid metal on a carrier, then cooled and heated the liquid metal for transfer it onto an elastomer layer [21]. The result is a relatively complex manufacturing process with many steps. In another method, manufacturers made masks with desired patterns and sprayed the liquid metal to completely cover the masked substrate [22]. While fast, the spraying of liquid metal on the mask resulted in waste of liquid metal and required manual post-processing and verification. In contrast, printing liquid metal patterns does not require premade molds or masks and does not rely as much on manual tuning of printing parameters. As a result, the printing method provides a simplified manufacturing process for sensors with different designs while also enabling a shorter manufacturing cycle.

We have classified the methods commonly used for printing liquid metal into three types: direct printing (i.e., using extrusion), printing with modified liquid metal, and contact printing (i.e., using a brush or ball that contacts the print surface). Various direct printing methods have been reported, including printing of liquid metal patterns on flat, inclined, and curved elastomer [17], printing of free standing liquid metal structures without the need for complex substrates [20], printing of liquid metal on metal electrodes for connecting eGaIn-based electronics to solid-state electronic devices

¹Department of Mechanical and Aerospace Engineering, UC San Diego, CA, USA. ²School of Engineering and Applied Sciences, Harvard University, MA, USA. ³Department of Mechanical Engineering, Seoul National University, Seoul, South Korea.

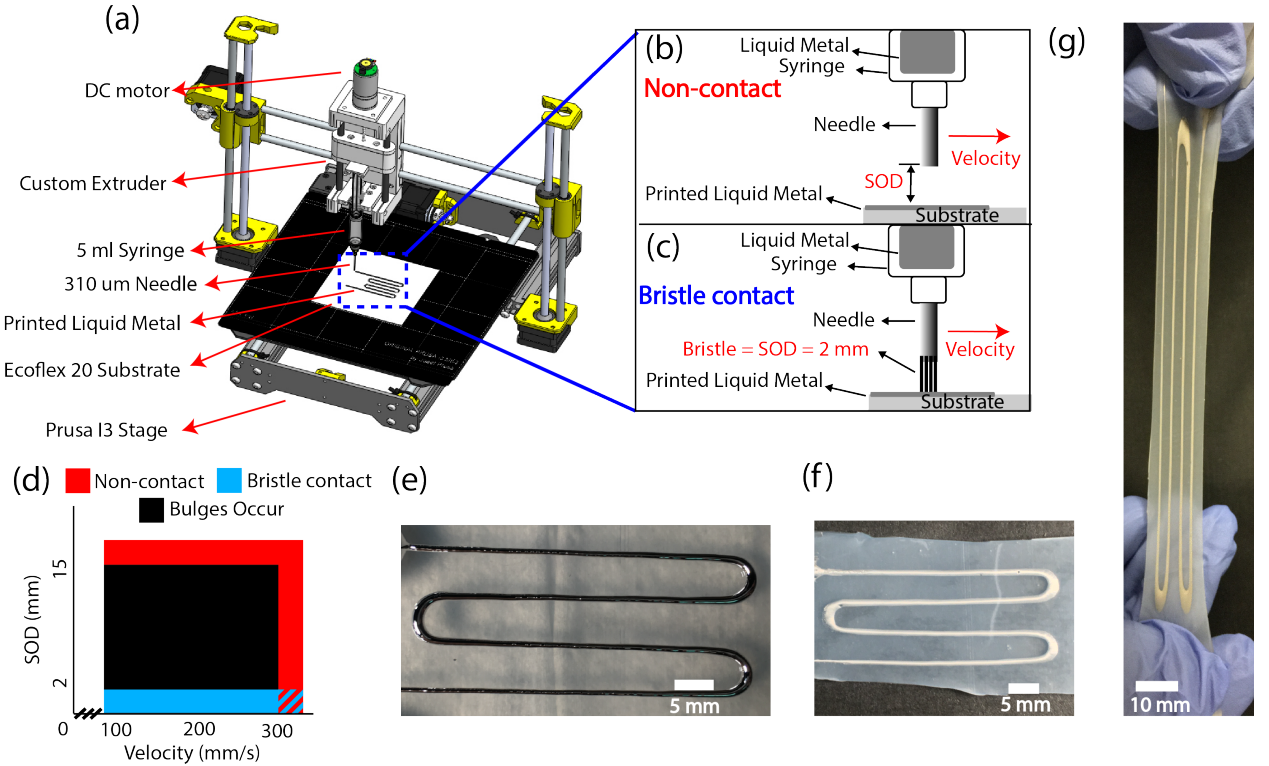


Fig. 1: Open-loop printing of liquid metal sensors. (a) Cartesian printer with a syringe mounted to a custom printhead used for extruding liquid metal through a blunt-nosed hypodermic needle. We propose a non-contact printing method where the needle is elevated from the substrate (b), as well as a contact method that uses bristles to maintain contact with the traces during printing (c). (d) Each method enables effective printing of liquid metal traces over a range of standoff distances (SOD) and print velocities with consistent trace thickness. The red and blue regions indicate parameter sets for which traces can be printed with consistent trace thickness for the non-contact and bristle contact methods, respectively. (e) Serpentine pattern printed in liquid metal using the bristle contact method. (f) Strain sensor made from encapsulating the printed liquid metal pattern in silicone rubber. (g) The resulting sensor was robust to 300% strain.

[19]. Printing methods that use modified liquid metal include electrowetting-assisted printing which applies voltage between liquid metal and substrate during extrusion [23], printing with laser-sintered liquid metal nanoparticles [24]–[27], and printing with paste-like modified liquid metal [28]. For contact printing, printing on specially selected paper using a ballpoint pen or a brush pen with liquid metal ink that has been oxidized by stirring for a specific period have been reported [29], [30].

Although these works can print consistent liquid metal patterns, they each have unsolved problems that should be addressed in order to increase the accessibility of printing liquid metal. Direct printing methods highly rely on precise feedback control of the print gantry. Previous work has demonstrated that the printer must use a stand-off distance (SOD) less than 0.3 mm, stage velocity less than 10 mm/s, and apply pressure less than 5 kPa to achieve successful printing [17]. Thus, direct printing methods have required sensors to maintain proper SOD during printing. Printing with modified liquid metal has required complex processes for modifying the ink. Although contact printing using ball pen or brush pen has been demonstrated to be faster and to place lower requirements on the SOD, they still require additional treatment of the liquid metal, and precise control

of the SOD during printing [29], [30]. Furthermore, these methods only work on select, paper-like materials that are flexible but not stretchable and are therefore poorly suited for making stretchable, liquid metal sensors.

In this work, we developed two methods for effectively printing continuous liquid metal patterns on stretchable substrates without the need for precise feedback control of SOD. The novelty of the proposed methods lies in their robustness to printing parameters enabling their use over a range of standoff distances and with higher stage velocities without the need to modify the liquid metal. The remainder of this paper is structured as follows. In the following section, we discuss the development of our printer and detail the experiments we used to characterize our proposed printing methods. In Section III, we present the results of our experiments and quantitatively compare the printing methods. In Section IV, we apply of soft strain sensors using our printing method. In Section V, we discuss our results in the broader context of manufacturing liquid metal sensors. Finally, we provide concluding remarks in Section VI.

II. MATERIALS AND METHODS

To test our proposed printing methods, we modified an open-source 3D printer (Prusa i3 MK3S+, Prusa Research) so that we could mount a custom syringe equipped with

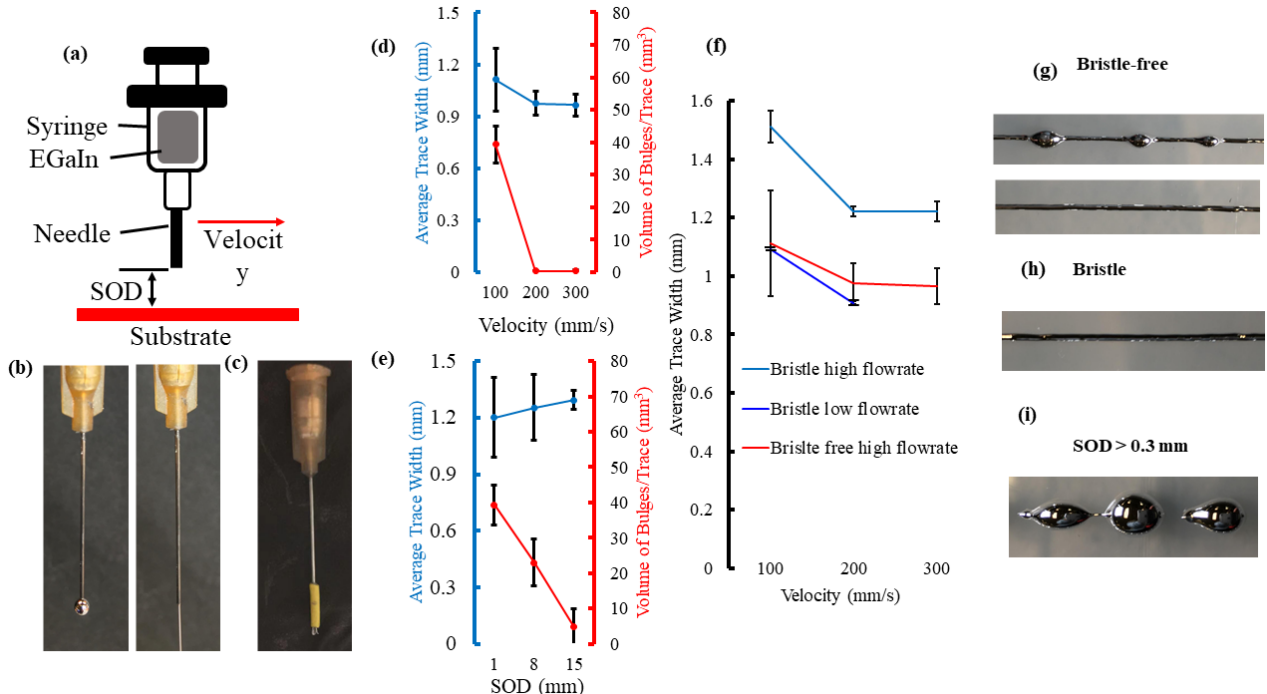


Fig. 2: Effects of printing speed and stand-off distance (SOD) on trace width. (a) Schematic of printhead with relevant printing parameters. (b) Left: liquid metal extruded as droplets using low flowrate of 0.68 ml/s. Right: liquid metal extruded as stream using high flowrate of 2.3 ml/s. (c) Stranded wire bristle attached at the tip of the needle. (d) Effect of stage velocity on trace width when printing with non-contact method, using a SOD of 2 mm. The variance of trace width and volume of bulges on traces decreased as the stage velocity increased. (e) Effect of varying SOD on trace width for non-contact method and a printhead velocity of 100 mm/s. The variance of trace width and volume of bulges on traces decreased as the SOD increased. (f) Comparison between non-contact and bristle contact method over varied velocity and flowrate. Unlike the non-contact method, the bristle contact method was able to print traces of consistent width using both low and high flowrates and a larger range of velocities. (g) Top: trace with high variance due to bulges from using the non-contact method with a stage velocity of 100 mm/s. Bottom: trace with low variance using the non-contact method with a velocity of 300 mm/s. (h) Trace with low variance printed by bristle contact method. (i) Failed trace printed using non-contact method with an SOD larger than 0.3 mm, a velocity of 10 mm/s, and a low flowrate. Sample size $n = 10$ for each experiment.

a blunt nosed hypodermic needle (inner diameter of 310 μm). The printer was controlled using open source motion control software (found at github.com/grbl/grbl) running on a commercially available microcontroller (Arduino Uno) equipped with a computerized numerical control (CNC) driver board (Arduino CNC shield V3, ACEIRMC). A major challenge with printing liquid metal is the high variability in the width of the printed traces due to periodic bulges that can occur along the traces. Previous work has mitigated this bulging with precise feedback control of the velocity of the stage, the pressure used for extrusion and the SOD [18]. We instead address this challenge using two open-loop approaches: 1) a non-contact method, which is a direct printing method that relies on quickly extruding streams of the liquid metal; and 2) a bristle contact method, which is a contact printing method that uses a set of bristles attached to the print head that act like a paint brush to maintain contact with the surface during the print, resulting in a consistent trace. Both of these approaches are used to maintain printing performance (i.e., variance of trace width) despite variation in the height of the substrate.

A. Printing Parameters

For both methods, we varied three parameters:

- Stage velocity – movement speed of the printhead
- Flowrate – flowrate of liquid metal from printer nozzle
- Stand-off distance (SOD) – distance between substrate and tip of the needle used to extrude the liquid metal

In this work, we used two flowrates, 0.68 ml/s and 2.3 ml/s. These flowrates were regulated using feedback control of the torque applied by the motor driving the syringe pump. The flowrate of 2.3 ml/s was chosen because it was the lowest flowrate that resulted in a stable stream of liquid metal for our printer (**Fig. 2b right**). The flowrate of 0.68 ml/s was chosen because it was the lowest possible flowrate for our printer and resulted in the liquid metal extruding as droplets (**Fig. 2b left**). For the bristle contact method, the SOD was set to the bristle length of 2 mm so that the bristle barely touched the substrate during the printing. Because we used a compliant syringe needle, the needle deformed whenever there was friction between the tip of the bristle and substrate. We leveraged this deformation to calibrate the SOD without a distance sensor. We calibrated the SOD by first placing

the needle tip at a height where we could observe contact between the bristle and the substrate. We then moved the printer head horizontally while lifting the printer head by steps of 0.1 mm until the needle no longer visibly deformed due to the friction.

B. Experimental Procedure

Among the most important factors in the design and fabrication of liquid metal sensors is the width of liquid metal traces. As the trace width is sensitive to variations in print parameters, it is necessary to characterize how these parameters affect the trace width. To find an appropriate set of parameters for both methods, we first tested the non-contact method by adjusting the stage velocity and the SOD with a constant flowrate. We then used a similar set of parameters to test the bristle contact method and compared the performance between the two methods. Next, we used a set of parameters which worked for both methods to study how well the proposed methods could resist changes in variation in height of substrates.

1) *Effect of parameters on non-contact method:* To test the effect of the stage velocity and the SOD on the non-contact method, we conducted two sets of experiments in which we only changed either the velocity or the SOD. We printed eight 100 mm long traces for each set of parameters and analyzed the average variance of the trace width and the volume of bulges forming along the printed traces. In both sets of experiments, we used a constant flowrate of 2.3 ml/s so that the liquid metal was extruded as a stream (**Fig. 2b**). Using lower flowrates resulted in discontinuities while printing the liquid metal traces (**Fig. 2i**). In the first set of experiments, we fixed the SOD at 2 mm and compared the print quality while using stage velocities of 100 mm/s, 200 mm/s, and 300 mm/s. We chose the stage velocity of 300 mm/s since it was the maximum velocity of the printer, and we chose velocities of 100 mm/s and 200 mm/s because they resulted in observable and meaningful differences in the quality of the liquid metal traces. In the second set of experiments, we fixed the stage velocity at 100 mm/s and compared the quality of the print as we adjusted the SOD to 1 mm, 8 mm, and 15 mm.

2) *Comparison between bristle contact and non-contact method:* To compare the performance of the non-contact and bristle contact methods, we set the SOD to 2 mm for both methods. Since the bristle contact method is capable of printing continuous liquid metal traces using both low and high flowrates, we tested the bristle contact method over various velocities (100 mm/s, 200 mm/s, and 300 mm/s) and flowrates (0.68 ml/s and 2.3 ml/s). We compared the print quality of both methods to demonstrate the bristle contact method's capacity to print with higher quality over a wider range of parameters. We printed eight 100 mm traces for each set of parameters and analyzed the average and variance of trace width.

3) *Effect of variation in height of substrates:* Previous work that printed liquid metals required precise control of SOD (i.e., to be <0.3 mm), meaning that any variation

in the height of the substrate would significantly affect the print quality. However, variations in the height of the substrate may be unavoidable and are highly dependant on the manufacturing process used to produce the substrate. To address this challenge, we characterized how robust our proposed methods were to variations in substrate height. This characterization also allowed us to test how well these methods could work on a non-planar surface without the need to adjust SOD during printing. We tested both print methods on substrates with designed variances in height. During printing, although we fixed the height of the extruder, the SOD changed due to the variation in the height of the substrate. We used a printhead velocity of 300 mm/s and a high flowrate of 2.3 ml/s for all the tests. We used both methods to print eight traces with decreasing (**Fig. 3c**) and increasing SOD (**Fig. 3d**). The printing started with SOD of 2 mm, and then the SOD was changed by steps of 0.8 mm, 0.6 mm, 0.4 mm, and 0.2 mm in each direction, for a total change of ± 2 mm.

III. RESULTS

A. Effect of parameters on non-contact method

The effects of the velocity of the stage and the SOD on the quality of the print are plotted in **Fig. 2d** and **Fig. 2e**, respectively. When we printed with a low SOD at 1 mm and a high flowrate (**Fig. 2d**), bulges of liquid metal formed when the velocity was not sufficiently high, leading to extra liquid metal printed on the traces. Increasing the stage velocity decreased the frequency of bulges in the liquid metal traces (**Fig. 2g**), resulting in lower variance in the trace width and lower volume of bulges. Using a SOD of 2 mm and high flowrate, the stage velocity was increased to 300 mm/s to print traces without bulges. When we printed with a low stage velocity at 100 mm/s and high flowrate (**Fig. 2e**), the volume of bulges decreased as we increased the SOD.

Therefore, when we printed with the non-contact method, it was possible to improve the print quality by increasing either the stage velocity or the SOD. With a stage velocity of 100 mm/s and high flowrate, an SOD of 15 mm was required to prevent the formation of bulges. Using low flowrates with the non-contact method resulted in an approach that was similar to previous printing methods. Without the feedback system used previously [17], we were unable to maintain an SOD smaller than 0.3 mm, resulting in discontinuous traces (**Fig. 2i**).

B. Comparison between bristle contact and non-contact method

As shown in **Fig. 2f**, when we used a high flowrate of 2.3 ml/s and low stage velocity of 100 mm/s, the bristle contact method resulted in traces with no notable bulging. In contrast, the non-contact method only resulted in traces with no bulging when a high stage velocity of 300 mm/s was used. However, traces printed using the bristle contact method had a larger average trace width since the traces were flattened by the bristles. In this case, trace width of liquid metal was largely effected by the bristle's shape. Furthermore, although

the non-contact method failed to print continuous traces using a low flowrate, the bristle contact method was able to print continuous traces without bulges using a low flowrate. At a low flowrate and stage velocity of 300 mm/s, the volume of extruded liquid metal was insufficient for printing continuous traces. Datapoints using these printing parameters were, therefore, omitted from all plots. In general, the bristle contact method could print continuous traces without bulging over a larger range of stage velocities and flowrates than the non-contact method as the bristles helped to smooth the traces and prevented bulges from forming during printing.

C. Effect of variation in height of substrates

For printing parameters that did not result in bulging, the mean and the variance of the trace width from both methods remained consistent as the SOD was varied (Fig. 3). As the SOD was decreased from 2 mm, the bristle contact method had a lower and more consistent variance in trace width than the non-contact method. This is attributed to the bristles contacting the substrate while printing, resulting in trace quality that did not diminish over the course of printing. As the SOD was increased from 2 mm, the variance in trace width for the bristle contact method was larger than that of the non-contact method. Since the printing started with a SOD that is the same as the length of the bristles, the latter lost contact with the liquid metal traces once the SOD increased. Without the bristles in contact, the printing worked similarly to the non-contact method. However, the bristles disturbed the extrusion of liquid metal, resulting in larger variance in trace width. For the non-contact method, the variation in SOD did not significantly change the average or variance of the traces. Thus, this approach demonstrated a larger tolerance in SOD compared to previous work, which required SODs smaller than 0.3 mm.

IV. APPLICATIONS

To verify whether the proposed methods were suitable for manufacturing sensors, we tested them by printing serpentine conductive patterns similar to those used previously in liquid metal strain sensors [12], [15], and calibrating the resulting strain sensors made with the bristle contact method.

A. Performance in printing serpentine strain patterns

We used a velocity of 300 mm/s, a constant high flowrate of 2.3 ml/s, and a SOD of 2 mm for both print methods. We chose this set of parameters as it prints continuous liquid metal trace without bulges for both methods. When we used the non-contact method to print a serpentine strain gauge pattern with length of 30 mm and gap width of 5 mm, bulges consistently formed around the corners of the pattern. As discussed above, the non-contact method required a high stage velocity in order to avoid printing traces with excessive bulging. Due to the physical limitations, our printer could not produce accelerations large enough to maintain a high stage velocity while turning around corners (Fig. 4b). To eliminate the bulges, we increased the gap width of the strain pattern from 5 mm to 10 mm (Fig. 4c). The curvature of the strain pattern was large enough to maintain a sufficiently

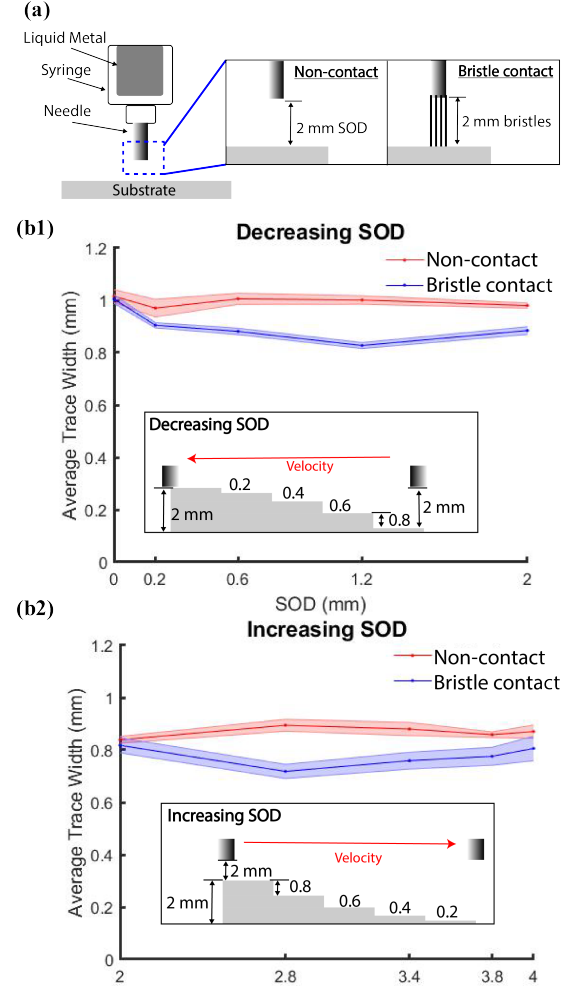


Fig. 3: Effects of varying substrate height on both open-loop print methods. (a) Schematic of syringe and needle using non-contact and bristle contact methods, with SOD set to bristle length (2 mm). The average width of traces as SOD is decreased (b1) and increased (b2) from a baseline of 2 mm. Shaded regions indicate one standard deviation of trace widths from the average trace width with a sample size of 10 traces. Insets in each plot indicate the order of heights in which the experiment was run.

large stage velocity to preventing bulges from forming during printing. Another method of eliminating bulging would be to use variable flowrate during the printing to extrude less liquid metal while printing corners [18], but this was not possible with our system. When using the bristle contact method to print the strain pattern with a length of 30 mm and a gap width of 5 mm, friction between the bristle and substrate led to the formation of bulges at the corners of the strain gauge pattern (Fig. 4d). This bulging is attributed to the compliance of the needle leading to both it and the bristles bending when the friction between the bristle and substrate became too large. This compliance led to the needle tip jamming on corners even while the extruder was moving. To solve this issue, we calibrated the printer such that the bristles lightly touched the substrate during printing (Fig.

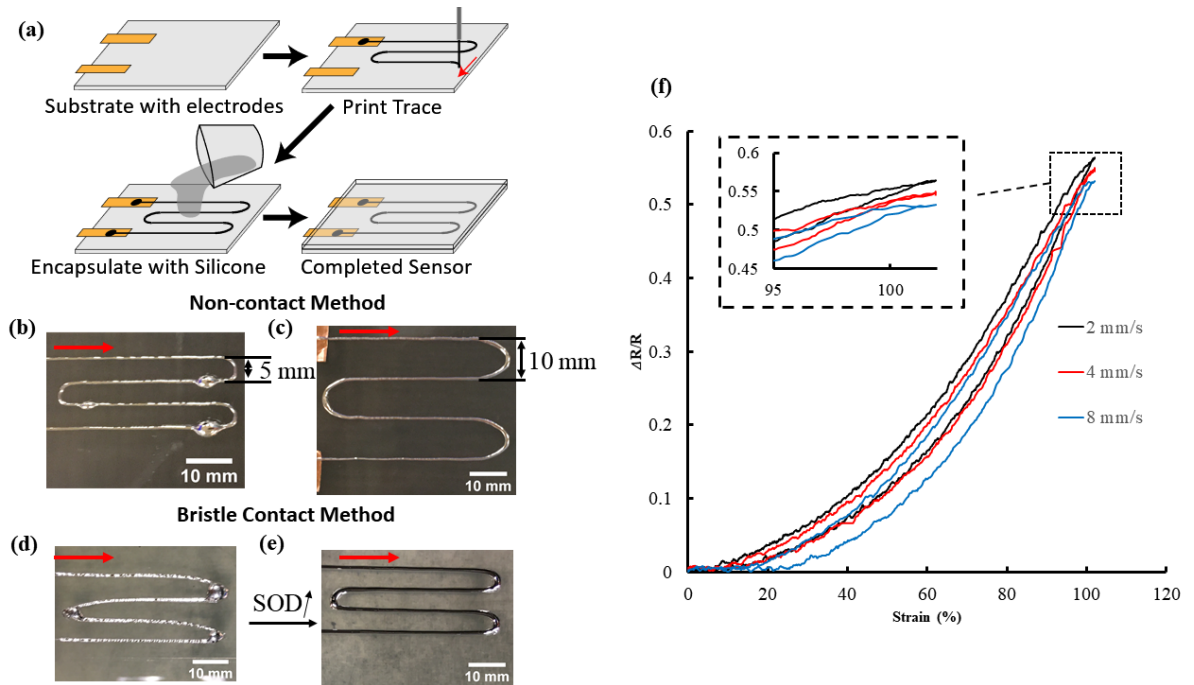


Fig. 4: Application of open-loop print methods to the fabrication of strain sensors. (a) Steps of manufacturing process for 3D printed liquid metal sensors.(b) Non-contact method printed bulges of liquid metal at corners of a strain gauge pattern with a 5 mm gap. (c) Bulging did not occur when the gap width was increased to 10 mm. (d) For low SOD with the bristle contact method, the needle bends when the bristles touch the substrate, causing the needle tip to stop around corners of a strain pattern with 5 mm gap width. (e) This is remedied by increasing the SOD to reduce friction between the needle and substrate. (f) Calibration result of strain sensor with different stretching speed.

4e). Other possible solutions include using a stiffer needle or constructing the bristle from a more compliant material that has less friction when sliding on silicone rubber.

B. Calibration of strain sensors

To verify that our printing method could manufacture functional sensors with performance similar to that from prior work, we made a strain sensor with a serpentine strain gauge pattern printed using the bristle contact method. After printing, we encapsulated the substrate and liquid metal with silicone rubber (Ecoflex 0020, Smooth-On Inc.). We then used a motorized stage (ESM750S, Mark-10) and force gauge (M7-50, Mark-10) to stretch the sensor up to 100% strain with speeds of 2 mm/s, 4 mm/s and 8 mm/s. The change in resistance of the sensor was approximately linear with respect to the strain and the overall response decreased slightly as the stretching speed increased (**Fig. 4f**). These behaviors were similar to those seen in strain sensors manufactured by injection-based methods [15].

V. DISCUSSION

The two open-loop print methods investigated in this work show promise for the low cost printing of liquid metal traces. The non-contact liquid metal printing method printed continuous and consistent liquid metal traces by using a combination of high extrusion flowrate (2.3 ml/s), a SOD less than 2 mm, and a stage velocity of 300 mm/s. When a high stage velocity was not achievable, a large SOD of 15 mm could be used instead to prevent the formation of

bulges. Compared to the non-contact method, the bristle contact method made it possible to print with a larger range of flowrates and stage velocities. Furthermore, we found that the bristles facilitate contact between the liquid metal and the soft substrate, helping to suppress bulges from forming over a larger range of flowrates. The non-contact method was able to maintain performance despite change of SOD up to 2 mm while the bristle contact method failed when the bristles lost contact with the liquid metal traces. Compared to previous printing methods, both methods tested here demonstrated larger tolerance to changes in the SOD, and the bristle contact method accommodated a wider range of stage velocities and flowrates. We also demonstrated the use of the bristle contact method to fabricate soft strain sensors. As a trade-off between precision and robustness, the proposed methods are not able to print micro-scale patterns like those presented in previous works that use high-precision sensors and low stage velocity. Furthermore, the resistance of the manufactured sensors varied slightly from sensor to sensor due to the open loop control of flowrate and SOD. It was possible for manufacturing errors from this open loop method to compound with variations in flowrate due to the material of syringe, the level of oxidation of the liquid metal, and the conditions inside the syringe, making it difficult to control the extruded volume of liquid metal. One major limitation of our printer was that it could only print with a constant flowrate. Future work could focus on using our open-loop printing methods with variable flowrate to create

strain sensors with smaller curvature. Further work could also focus on optimizing the design of the bristles used in our contact method, adjusting parameters like the material, length, and number of bristles. Finally, future work could study system parameters that could be adjusted to control the width of the printed traces.

VI. CONCLUSION

In summary, our two proposed printing methods provided open-loop approaches for fabrication of liquid metal sensors. We characterized the print quality of each method as a function of the printing parameters, such as SOD, stage velocity, and flowrate, and demonstrated that sensors developed using our methods performed similarly to those from previous work. Both of our proposed methods were demonstrated to print liquid metal traces at stage velocities up to 300 mm/s. However, we found that between our two open-loop methods, the bristle contact method printed traces with smaller variance in trace width as long as contact between the bristles and the substrate was maintained. Compared to previous work in printing liquid metal sensors, our methods significantly accelerate the printing of liquid metal on stretchable substrates while allowing for greater variance in the manufacturing of those substrates.

ACKNOWLEDGEMENT

This work was supported by the Office of Naval Research, grant numbers N00014-17-1-2062 and N00014-18-1-2277. The authors would like to thank Yaoting Xue for his help in formulating the liquid metal compound used in this work.

REFERENCES

- [1] H. Shi, M. Al-Rubaiai, C. M. Holbrook, J. Miao, T. Pinto, C. Wang, and X. Tan, "Screen-printed soft capacitive sensors for spatial mapping of both positive and negative pressures," *Advanced Functional Materials*, vol. 29, no. 23, p. 1809116, 2019.
- [2] O. Atalay, A. Atalay, J. Gafford, and C. Walsh, "A highly sensitive capacitive-based soft pressure sensor based on a conductive fabric and a microporous dielectric layer," *Advanced Materials Technologies*, vol. 3, no. 1, p. 1700237, 2018.
- [3] R. P. Rocha, P. A. Lopes, A. T. de Almeida, M. Tavakoli, and C. Majidi, "Fabrication and characterization of bending and pressure sensors for a soft prosthetic hand," *Journal of Micromechanics and Microengineering*, vol. 28, no. 3, p. 034001, 2018.
- [4] B. Shih, D. Drotman, C. Christianson, Z. Huo, R. White, H. I. Christensen, and M. T. Tolley, "Custom soft robotic gripper sensor skins for haptic object visualization," in *2017 IEEE/RSJ IROS*, pp. 494–501.
- [5] J. Guo, X. Liu, N. Jiang, A. K. Yetisen, H. Yuk, C. Yang, A. Khademhosseini, X. Zhao, and S.-H. Yun, "Highly stretchable, strain sensing hydrogel optical fibers," *Advanced Materials*, vol. 28, no. 46, pp. 10244–10249, 2016.
- [6] P. A. Xu, A. K. Mishra, H. Bai, C. A. Aubin, L. Zullo, and R. F. Shepherd, "Optical lace for synthetic afferent neural networks," *Science Robotics*, vol. 4, no. 34, 2019.
- [7] E. Roh, B.-U. Hwang, D. Kim, B.-Y. Kim, and N.-E. Lee, "Stretchable, transparent, ultrasensitive, and patchable strain sensor for human-machine interfaces comprising a nanohybrid of carbon nanotubes and conductive elastomers," *ACS Nano*, vol. 9, no. 6, pp. 6252–6261, 2015.
- [8] S. Lee, A. Reuveny, J. Reeder, S. Lee, H. Jin, Q. Liu, T. Yokota, T. Sekitani, T. Isayama, Y. Abe, *et al.*, "A transparent bending-insensitive pressure sensor," *Nature Nanotechnology*, vol. 11, no. 5, pp. 472–478, 2016.
- [9] B. Shih, J. Mayeda, Z. Huo, C. Christianson, and M. T. Tolley, "3d printed resistive soft sensors," in *2018 IEEE International Conference on Soft Robotics (RoboSoft)*, pp. 152–157, IEEE, 2018.
- [10] Y. Wang, Y. Lu, D. Mei, and G. Qiang, "Development of wearable tactile sensor based on galinstan liquid metal for both temperature and contact force sensing," in *2020 IEEE 16th International Conference on Automation Science and Engineering (CASE)*, pp. 442–448, IEEE, 2020.
- [11] B. Shih, D. Shah, J. Li, T. G. Thuruthel, Y.-L. Park, F. Iida, Z. Bao, R. Kramer-Bottiglio, and M. T. Tolley, "Electronic skins and machine learning for intelligent soft robots," *Science Robotics*, vol. 5, no. 41, 2020.
- [12] B. Shih, E. Lathrop, I. Adibnazari, R. Martin, Y.-L. Park, and M. T. Tolley, "Classification of components of affective touch using rapidly-manufacturable soft sensor skins," in *2020 3rd IEEE International Conference on Soft Robotics (RoboSoft)*, pp. 182–187, IEEE, 2020.
- [13] T. G. Thuruthel, B. Shih, C. Laschi, and M. T. Tolley, "Soft robot perception using embedded soft sensors and recurrent neural networks," *Science Robotics*, vol. 4, no. 26, p. eaav1488, 2019.
- [14] T. Kim and Y.-L. Park, "A soft three-axis load cell using liquid-filled three-dimensional microchannels in a highly deformable elastomer," *IEEE Robotics and Automation Letters*, vol. 3, no. 2, pp. 881–887, 2018.
- [15] Y.-L. Park, B.-R. Chen, and R. J. Wood, "Design and fabrication of soft artificial skin using embedded microchannels and liquid conductors," *IEEE Sensors Journal*, vol. 12, no. 8, pp. 2711–2718, 2012.
- [16] J. Oh, S. Kim, S. Lee, S. Jeong, S. H. Ko, and J. Bae, "A liquid metal based multimodal sensor and haptic feedback device for thermal and tactile sensation generation in virtual reality," *Advanced Functional Materials*, p. 2007772, 2020.
- [17] G. Shin, B. Jeon, and Y.-L. Park, "Direct printing of sub-30 m liquid metal patterns on three-dimensional surfaces for stretchable electronics," *Journal of Micromechanics and Microengineering*, vol. 30, no. 3, p. 034001, 2020.
- [18] S. Kim, J. Oh, D. Jeong, W. Park, and J. Bae, "Consistent and reproducible direct ink writing of eutectic gallium-indium for high-quality soft sensors," *Soft robotics*, vol. 5, no. 5, pp. 601–612, 2018.
- [19] S. Kim, J. Oh, D. Jeong, and J. Bae, "Direct wiring of eutectic gallium-indium to a metal electrode for soft sensor systems," *ACS Applied Materials & Interfaces*, vol. 11, no. 22, pp. 20557–20565, 2019.
- [20] C. Ladd, J.-H. So, J. Muth, and M. D. Dickey, "3d printing of free standing liquid metal microstructures," *Advanced Materials*, vol. 25, no. 36, pp. 5081–5085, 2013.
- [21] T. Kim, D.-m. Kim, B. J. Lee, and J. Lee, "Soft and deformable sensors based on liquid metals," *Sensors*, vol. 19, no. 19, p. 4250, 2019.
- [22] R. Guo, L. Sheng, H. Gong, and J. Liu, "Liquid metal spiral coil enabled soft electromagnetic actuator," *Science China Technological Sciences*, vol. 61, no. 4, pp. 516–521, 2018.
- [23] A. M. Watson, A. B. Cook, and C. E. Tabor, "Electrowetting-assisted selective printing of liquid metal," *Advanced Engineering Materials*, vol. 21, no. 10, p. 1900397, 2019.
- [24] E. L. White, J. C. Case, and R. K. Kramer, "Reconfigurable logic devices connected with laser-sintered liquid metal nanoparticles," in *2017 IEEE SENSORS*, pp. 1–3, IEEE, 2017.
- [25] S. Liu, M. C. Yuen, and R. Kramer-Bottiglio, "Reconfigurable electronic devices enabled by laser-sintered liquid metal nanoparticles," *Flexible and Printed Electronics*, vol. 4, no. 1, p. 015004, 2019.
- [26] S. Liu, M. C. Yuen, E. L. White, J. W. Boley, B. Deng, G. J. Cheng, and R. Kramer-Bottiglio, "Laser sintering of liquid metal nanoparticles for scalable manufacturing of soft and flexible electronics," *ACS Applied Materials & Interfaces*, vol. 10, no. 33, pp. 28232–28241, 2018.
- [27] S. Liu, S. N. Reed, M. J. Higgins, M. S. Titus, and R. Kramer-Bottiglio, "Oxide rupture-induced conductivity in liquid metal nanoparticles by laser and thermal sintering," *Nanoscale*, vol. 11, no. 38, pp. 17615–17629, 2019.
- [28] U. Daalkhaijav, O. D. Yirmibesoglu, S. Walker, and Y. Mengüç, "Rheological modification of liquid metal for additive manufacturing of stretchable electronics," *Advanced Materials Technologies*, vol. 3, no. 4, p. 1700351, 2018.
- [29] Y. Zheng, Z.-Z. He, J. Yang, and J. Liu, "Personal electronics printing via tapping mode composite liquid metal ink delivery and adhesion mechanism," *Scientific Reports*, vol. 4, no. 1, pp. 1–8, 2014.
- [30] Y. Zheng, Z. He, Y. Gao, and J. Liu, "Direct desktop printed-circuits-on-paper flexible electronics," *Scientific Reports*, vol. 3, no. 1, pp. 1–7, 2013.